Optimization of the Electric Field Distribution induced in the Brain during Transcranial Magnetic Stimulation (TMS) using the Continuum Design Sensitivity Analysis (CDSA)

DONG-HUN KIM[1], G. E. GEORGHIOU[2], JONG-WOO CHOI[1], WON-EEL YUN[1]
[1]School of Electrical Engineering and Computer Science
Kyungpook National University
Daegu, 702-701
KOREA

[2]School of Electronic and Computer Science
University of Southampton
Southampton, SO17 1BJ
UNITED KINGDOM

Abstract: - Results are presented on the optimization of the electric field distribution obtained during Transcranial Magnetic Stimulation (TMS) for deep neuron stimulation by using the Continuum Design Sensitivity Analysis (CDSA) combined with a commercially available generalized finite element code (OPERA). In order to obtain a magnetic field that can penetrate deeply and safely to activate the brain's central structures, an iron core is introduced and its shape is optimized, as opposed to searching for a combination of several coils that make both the analysis and construction of such a design very complex. It is revealed that the introduction of an optimized iron core enhances the magnitude and localization of the electric field induced inside the brain when compared with conventional coil structures.

Key-Words: - Design sensitivity analysis, Field localization, Finite element method, Induced electric field, Transcranial magnetic stimulation.

1 Introduction

Considerable research on magnetic stimulation of the human brain through Transcranial Magnetic Stimulation (TMS) has been carried out in the past few years due to its demonstrated ability to activate specified areas of the nervous system and the non-invasive nature of the stimulation [1-4]. Most of the effort has recently focused on an attempt to improve the design of the stimulating coil that is necessary for deep penetration and localized distribution of the fields inside the brain mass.

Existing designs of stimulating coil configurations are somewhat crude and their energy efficiency of coupling to the brain are very low because the TMS stimulator in all cases is made out of a wire-wound coil, typically circular or in the shape of the figure of eight, or variations of these [3, 4], placed against the scalp. As a result, there is a need for new TMS coil configurations to generate sufficient and localized electric fields to achieve deep stimulation.

As part of the search for new TMS coil configurations, the authors have already examined the effects of the geometrical models of the head on the distribution and penetration of the electric field induced in the brain. Moreover, the advantages of using a properly designed iron core for short operating times of typical TMS operation (50-200 μs) have been demonstrated by revealing increased maximum field strength induced inside the brain in the presence of the iron core in the range 50-70 V/m [5].

This paper presents results on the optimization of the distribution and penetration of the electric field induced inside the brain during the TMS. To obtain sufficient and localized electric fields inside the brain, an iron core is introduced and its shape is optimized using the Continuum Design Sensitivity Analysis (CDSA) combined with the Finite Element Method (FEM) [6, 7]. Finally the results obtained with the optimised coil are compared with those obtained from coil designs employed in commercial TMS stimulators, namely the butterfly-shaped coil and the three-loop slinky coil, demonstrating enhanced performance in terms of magnitude and localization of the electric fields induced inside the brain.

2 Analytical Sensitivity Formula

Under the assumption of the quasi-static approximation of the electric fields generated inside the brain at low frequencies and linear material properties, an analytical sensitivity formula for steady state eddy current problems is developed. A detailed expansion of the formula is omitted here since it is somewhat complicated but otherwise a fairly routine process [6, 7]. Fig. 1 illustrates the conversion relationship of the dual system of the CDSA in eddy current problems, which consists of the primary and the adjoint systems.

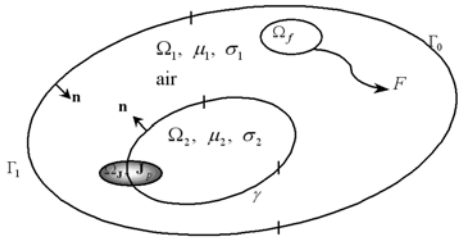

(a)

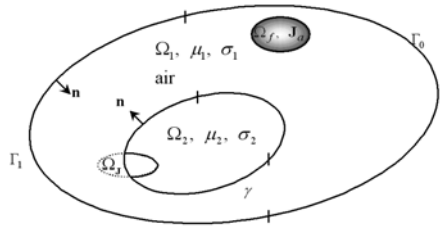

(b)

Fig. 1 Dual system of the CDSA: (a) primary system, (b) adjoint system.

In the primary system shown in Fig. 1(a), the optimization problem of adjustment of a local quantity distribution such as the electric field or eddy current in the region of interest, Ω_f is mathematically formulated as shown in equations (1)-(3).

We minimize

$$F = \int_{\Omega_f} f(\mathbf{A}_1)\, d\Omega \tag{1}$$

subject to

$$-\nabla\times(\upsilon\nabla\times\mathbf{A}) - j\omega\sigma\mathbf{A} + \mathbf{J}_s = 0 \quad \text{in } \Omega_1, \Omega_2 \tag{2}$$

$$\mathbf{n}\cdot(\nabla\times\mathbf{A}_2 - \nabla\times\mathbf{A}_1) = 0,$$

$$\mathbf{n}\times(\upsilon_2\nabla\times\mathbf{A}_2 - \upsilon_1\nabla\times\mathbf{A}_1) = 0 \quad \text{on } \gamma \tag{3}$$

where the subscripts, 1 and 2, denote different material regions where the physical quantities are defined, respectively. In equation (1), f is an arbitrary scalar function differentiable with respect to **A**. The argument A of the objective function F representing a design goal must satisfy the system equation (2) with the interface boundary condition, equation (3), on γ, which describes the primary system depicted in Fig. 1(a).

To obtain an explicit expression for the variation of equation (1) with respect to the design variables, the material derivative concept of continuum mechanics and some mathematical manipulations are applied to the augmented objective function including the objective function (1) and the equality constraints, (2) and (3). An adjoint system shown in Fig. 1(b)– the counterpart of the primary system – is systematically derived during the procedure mentioned above [6, 7]. This gives

$$-\nabla\times(\upsilon\nabla\times\boldsymbol{\lambda}) - j\omega\sigma\boldsymbol{\lambda} + \mathbf{f}_1 = 0 \quad \text{in } \Omega_1, \Omega_2 \tag{4}$$

$$\mathbf{n}\cdot(\nabla\times\boldsymbol{\lambda}_2 - \nabla\times\boldsymbol{\lambda}_1) = 0,$$

$$\mathbf{n}\times(\upsilon_2\nabla\times\boldsymbol{\lambda}_2 - \upsilon_1\nabla\times\boldsymbol{\lambda}_1) = 0 \quad \text{on } \gamma \tag{5}$$

where $\mathbf{f}_1 = [\partial f/\partial A_x,\ \partial f/\partial A_y,\ \partial f/\partial A_z]$ represents the pseudo electric current in the adjoint system and $\boldsymbol{\lambda}$ is the complex vector interpreted as the adjoint variable. The above adjoint system is the core of the CDSA as the design sensitivity is computed ultimately by using **A** and $\boldsymbol{\lambda}$.

Finally, the continuum sensitivity formula takes the surface integration form along the movable part of γ, which is assigned for the design variables:

$$dF/d\mathbf{p} = \int_\gamma [(\upsilon_1 - \upsilon_2)\nabla\times\mathbf{A}_1\cdot\nabla\times\boldsymbol{\lambda}_2 +$$

$$j\omega(\sigma_1 - \sigma_2)\mathbf{A}_1\cdot\boldsymbol{\lambda}_2 - (\mathbf{J}_1 - \mathbf{J}_2)\cdot\boldsymbol{\lambda}_1]\mathbf{n}\, d\Gamma \tag{6}$$

where **p** is a vector of design variables and **n** is the unit vector normal to the interface where p is defined. The three integrands on the right-hand side of equation (6) contribute to the sensitivity coefficients only when the design variables experience the difference of permeability, conductivity and current density across the interface boundary γ.

3 Implementation of Standard EM Software as a design tool

The derived formula, equation (6), combined with a general FEM software, such as OPERA in this case, is used to compute the design sensitivity, which represents the first-order derivative of the objective function. The program architecture consisting of two independent modules as shown in Fig. 2 is employed. The Optimization Module controls the overall design procedure and evaluates crucial quantities such as the objective function, adjoint load term, and design

sensitivity. This module generates two important data files, which store updated information about the changes of the design variables and the adjoint load. The purpose of the Analysis Module is to estimate the performance of the dual system at each design stage and to execute the command files that include the complete specification of the design model. When changes to the design variables and adjoint loads are uploaded into the two data files at each iterative design process, the command file reads the improved design information from the data files using the user input/output commands offered by the software package. The Analysis Module can contain any commercial EM software as long as the commands used are compatible with the software. It should be noted that the two modules are constantly communicating with each other and exchanging information about design variables, regions of interest and state variables through the data/output files.

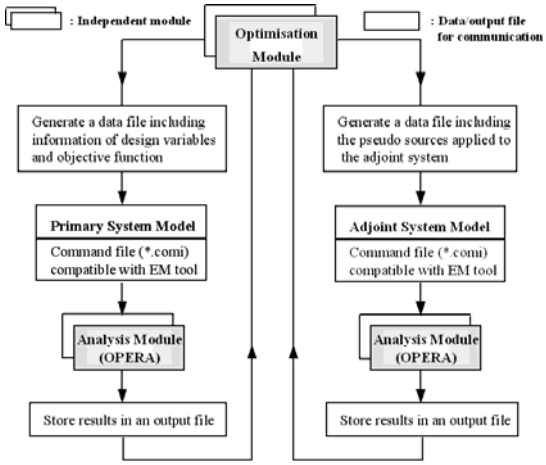

Fig. 2 Program architecture for design optimisation.

The sensitivity coefficients are evaluated from the analytical formula, equation (6), using the two post-processing output files of the dual system. The flow of the optimization algorithm can thus be summarized as follows:

(I) Read updated information about design variables through the command file of the Primary System Model;

(II) Solve the primary system for the state variable A by the Analysis Module;

(III) Take the post-processing data of the primary system and then calculate the objective function *F* and adjoint load term f_1 in the Optimization Module;

(IV) Read the updated adjoint load through the command file of the Adjoint System Model;

(V) Solve the adjoint system for the adjoint variable λ by the Analysis Module;

(VI) Take the post-processing data of the adjoint system and then compute the sensitivity coefficient by numerical surface integration of the sensitivity formula in the Optimization Module.

The above design process is repeated until the objective function converges to the optimum solution.

4 Results

In order to obtain sufficient and localized electric field inside the brain, an iron core inserted into the stimulus coil is thought to be the best choice in terms of degree of focusing, combined with simplicity and ease of use, rather than searching for a combination of several coils such as the slinky coil, butterfly coils etc, used by other authors [3, 4]. The shape of an iron core is optimized in terms of increasing and localizing the electric field induced by the single-loop stimulating coil using the CDSA combined with the OPERA axisymmetric steady state solver. Thereafter a practical core, deduced from the optimized one with considerations of manufacturing constraints, is applied to a butterfly-shaped coil of two loops as well as a single-loop coil and their field distributions are compared with those of the conventional coil combinations by using the OPERA 3d steady state solver.

4.1 Shape optimization of the iron core

For the sake of saving design time, an optimization problem presented here is conducted with the traditional sphere head model (HM1) and a single-loop stimulating coil. By means of the FE simulation, it is ascertained that the electric field generated by a stimulus coil with a cylindrical core (without any use of optimization) shown in Fig. 3 is increased by nearly two times compared to the coreless coil. This is effectively caused by the increase in flux linkage passed through the coil. However, in order to penetrate and concentrate the field deeply and locally into the brain, the optimum shape of the iron core is still required. To achieve this, the optimization algorithm described earlier is applied to the initial design model with the traditional sphere head model (HM1) of radius 10 cm as shown in Fig. 3, where the effective centre of the coil is 4.0 cm above the vertex of the head. The stimulator consists of a 30-turn circular coil with a cross section of 1.0 cm × 1.0 cm

and effective radius of 2 cm. The coil is excited with an amplitude of 1 A and frequency of 10 kHz. The homogeneous and isotropic conductivity of 0.4 S/m is assumed here.

The design goal is to produce the required electric field distributed over the 15 objective regions, which is chosen to be stronger by 30% than the initial field distribution and to have the maximum field position shifted towards the centre of the coil by 5 mm (refer to Fig. 4(c)). To achieve this goal, the objective function was mathematically expressed in terms of eddy current loss and evaluated over the 15 objective regions as follows:

$$F = \sum_{j=1}^{15} (P_j - P_{jo})^2 \Omega_{ej}, \quad P_j = \int_{\Omega_{ef}} \frac{1}{\sigma} \mathbf{J}_e \cdot \mathbf{J}_e^* \, d\Omega \quad (7)$$

where P_j and P_{jo} are the eddy current loss and target value generated in the *j*-th objective region, respectively. Ω_{ej} denotes the area of the *j*-th objective region and $\mathbf{J}_e$ means the eddy current vector. In this case, the pseudo source in the adjoint system appeared in equation (4) is defined as:

$$\mathbf{f}_1 = -j\omega \mathbf{J}_e^* \quad (8)$$

where ω is a angular frequency and * means a conjugate vector.

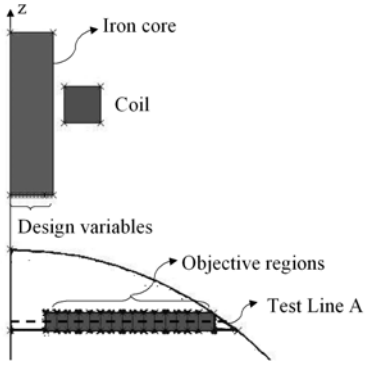

Fig. 3 Initial design model.

A total of 13 grid points forming the bottom line of the core are selected as design variables and allowed to move in the y and z-axis. To facilitate the conformity of the FE mesh with the continued shape changes of the design during the optimization process, the z directional movement of individual design variable is limited to 5 mm from the perimeter of HM1.

After 11 iterations, the optimal core shape was obtained and compared with the initial one in Fig. 4(a). Taking into account manufacturing constraints, a practical core is deduced as shown in Fig. 4(b) based on the optimized shape. Fig. 4(c) illustrates the optimized and practical core field distribution, which is approximately 30% stronger than the initial one. Furthermore, the maximum field position shifts by 3 mm compared with the initial core. This result clearly demonstrates that the electric field distribution induced inside the brain during TMS can be controlled in terms of magnitude and localization by using a well-designed iron core.

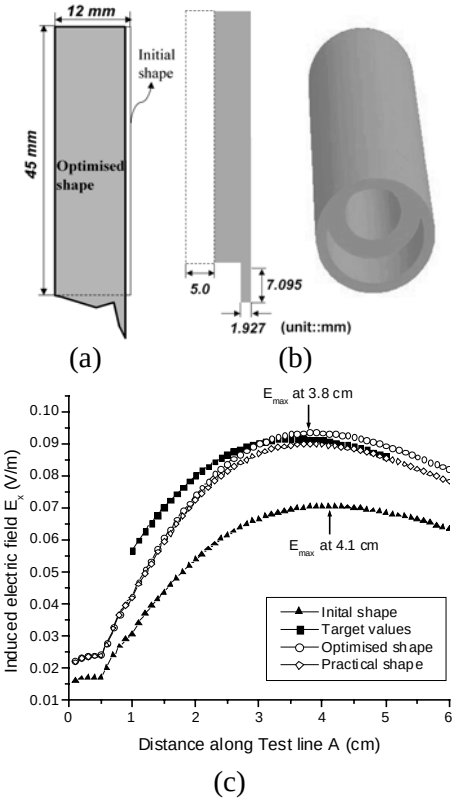

Fig. 4 (a) Optimized core shape, (b) practical core shape, (c) comparison of the induced electric field along Test line A. (angular frequency ωt=90^o).

4.2 Comparison of the field distribution between different stimulators

The optimized practical iron core is now used in conjunction with a second head model (HM2) incorporating different radii along the three axes as shown in Fig. 5. Fig. 5(a) shows the induced electric field distribution over the surface of HM2 when the effective centre of the coil is 2.0 cm above the vertex of the head and when the coil with the core is tilted by 25^o against the rotating axis parallel to the x-axis and passing through the centre of the brain located at (0,0,-12 cm). It can be seen that the presence of ears in the head model affects the flow of the induced fields on the surface of the head. The effect of the optimized practical iron core on the induced field distribution

along the two test lines depicted in Fig. 5(b) is presented in Fig. 6 for HM2 where a major component of the electric field induced along the two test lines is parallel to the x-axis. The practical core causes a field increase of more than 230% in terms of maximum value of the fields, compared to the coreless coil.

The single-loop coil is then replaced by a two-loop coil widely used in commercial devices. This stimulator consists of a butterfly-shaped coil with a driving current in opposite direction and each coil plane located at 2 above the vertex of the head. Fig. 7 shows two conventional coil assemblies referred to as a butterfly-shaped coil of two loops and a three-loop Slinky coil. A butterfly-shaped coil with the optimized core is also shown. Their induced electric field distributions over the surface of HM2 also appear in Fig. 7. The localization of the induced fields is assessed by the half-power region (HPR), which is defined as the region within which the magnitude of the normalized field is greater than about 0.7. Fig. 8 presents the comparison of the field localization and magnitude between the three different stimulators along the two test lines. It can be seen that the butterfly-shaped coil with the optimized practical core (Fig. 7(c)) produces a field increase of more than two times in terms of maximum value of the fields, while it helps to slightly improve the field localization, compared to the butterfly-shaped coil without the core (Fig. 7(a)).

5 Conclusion

In this paper an optimized practical iron core for effective TMS of the brain has been presented. Two different geometrical head models and conventional coil combinations were considered in order to validate the use of the optimized core. The CDSA is used to establish an optimized practical core for a single-loop stimulating coil to enhance the magnitude and localization of the electric field induced inside the brain. The optimized practical core applied to a single-loop and a butterfly-shaped coil is shown to lead to increased energy efficiency of coupling to the brain, induced field magnitude and field localization

Work is under way towards an improved TMS stimulation coil structure that can enhance the localization as well as the magnitude of the electric field.

Acknowledgment

This research was supported by Kyungpook National University Research Fund, 2004.

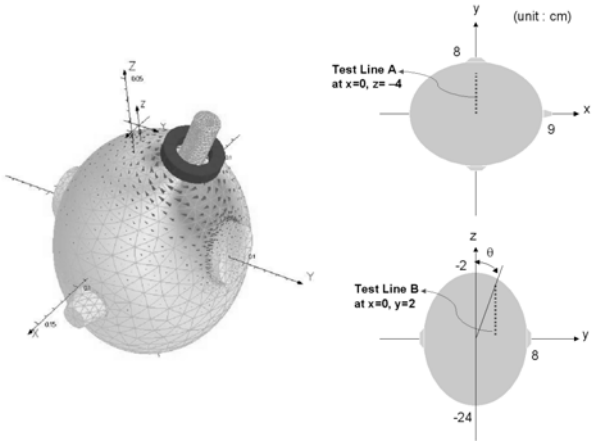

(a) (b)

Fig. 5 (a) Head Model HM2 and the induced electric field distribution, (b) lateral views of HM2.

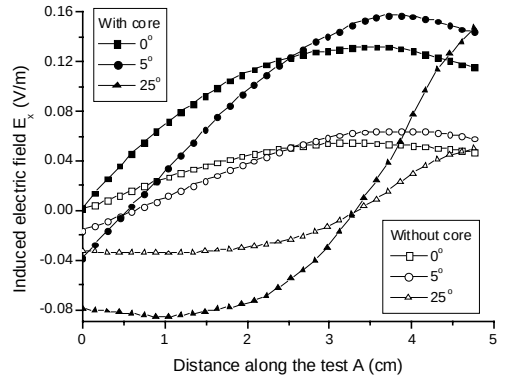

(a)

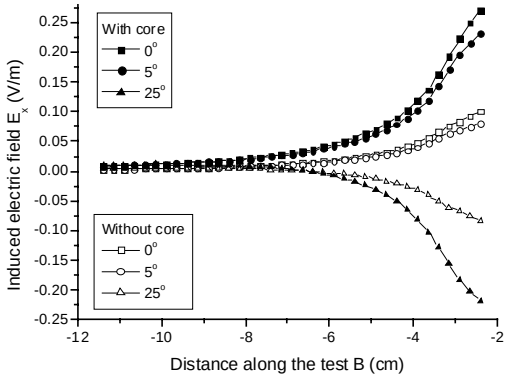

(b)

Fig. 6 Comparison of the induced current density distributions between the coreless coil and the practical core for HM2 ($\omega t=90^{o}$): (a) along Test line A (b) along Test line B.

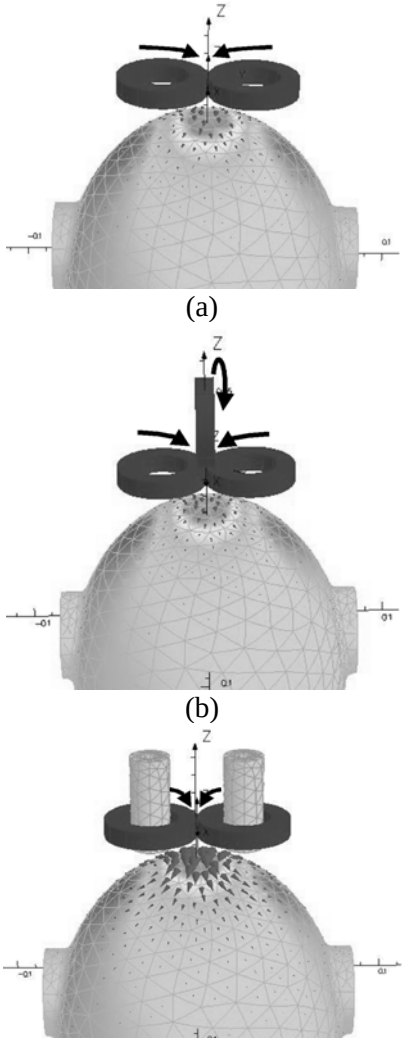

Fig. 7 Comparison of the induced current density distributions on the surface between three different coil assemblies for HM2: (a) a butterfly-shaped coil of two loops without the core, (b) a three-loop Slinky coil, (c) a butterfly-shaped coil of two loops with the practical core.

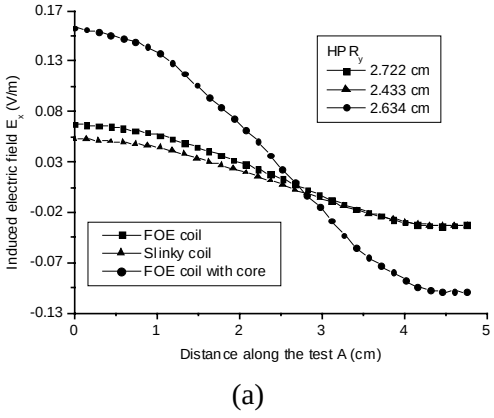

(a)

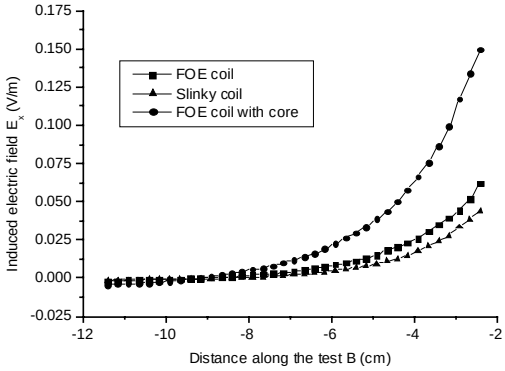

(b)

Fig. 8 Comparison of the induced current density distributions and localization between three different coil assemblies for HM2 ($\omega t=270^{o}$): (a) along Test line A, (b) along Test line B.

References

[1] Pedro C. Miranda, Mark Hallett and Peter J. Basser, *The electric field induced in the brain by magnetic stimulation: A 3-D finite-element analysis of the effect of tissue heterogeneity and anisotropy*, *IEEE Trans. Biomed. Eng*., Vol. 50, . 2003, pp. 1074-1085

[2] Jacek Starzynski, Bartosz Sawicki, Stanislaw Wincenciak, Andrzej Krawczyk and Tomasz Zyss, *Simulation of magnetic stimulation of the brain*, *IEEE Trans. Magn.*, Vol. 38, 2002, pp. 1237-1240.

[3] Chunye Ren, Peter P. Tarjan and Dejan B. Popovic, *A novel electric design for electromagnetic stimulation-The slinky coil*, *IEEE Trans. Biomed. Eng.*, Vol. 42, 1995, pp. 918-925.

[4] Kai-Hsiung Hsu and Dominique M. Durand, *A 3-D differential coil design for localized magnetic stimulation*, *IEEE Trans. Biomed. Eng*., Vol. 48, 2001, pp. 1162-1168.

[5] Dong-Hun Kim, N. Loucaides, J. K. Sykulski and G. E. Georghiou, *Numerical investigation of the electric field distribution induced in the brain by TMS*, Accepted for Publication in IEE Proc. Science Measurement and Technology, 2004

[6] Dong-Hun Kim, Il-Han Park, Myoung-Chul Shin and J. K. Sykulski, *Generalized continuum sensitivity formula for optimum design of electrode and dielectric contours*, *IEEE Trans Magn*, Vol. 39, 2003, pp. 1281-1284.

[7] Dong-Hun Kim, Se-Hee Lee, Il-Han Park and Joon-Ho Lee, *Derivation of a general sensitivity formula for shape optimization of 2D magnetostatic systems by continuum approach*, *IEEE Trans Magn*, Vol. 38, 2002, pp. 1125-1128.